Aust. J. Phys., 1985, **38**, 971–4

Evidence for a Common Magnetic Driver for Flares and Quiescent Coronae/Chromospheres*

A. Skumanich

High Altitude Observatory,
National Center for Atmospheric Research,
P.O. Box 3000, Boulder, CO 80307, U.S.A.

Abstract

The mean power and rate of optical flares in dMe stars are found to be correlated with their *quiet* coronal X-ray luminosity. The mean flare luminosity in the photometric U-band appears to scale *linearly* with the X-ray luminosity with a slope of 0·04. This coincidence suggests that quiet and flare activity in coronae/chromospheres may be related by one and the same flaring mechanism. We propose that 'quiet' activity is due to microflares—a low yield but high frequency continuation of flares.

1. Introduction

Given Ron Giovanelli's interest in magnetic activity and reconnection on the Sun, undoubtedly his attention would have turned sooner or later to what is now called the solar–stellar connection, i.e. the study of solar-like phenomena in other stars. Consequently, it is appropriate to present some speculative comments about optical flares on dMe stars and their relation to their quiet coronae.

2. Analysis

In a landmark paper on flares in dMe stars, Lacy, Moffett and Evans (1976; here referred to as LME) presented a correlation between the mean flare power or luminosity $\dot{Y}_{\mathrm{U}}$ in the photometric U-band, centred on λ 3500 Å, and the photospheric U-band luminosity L_{U}. They found that $\dot{Y}_{\mathrm{U}} \approx L_{\mathrm{U}}^{2/3}$. I would like to suggest that their relation reduces to a simpler and more physically meaningful relation if the quiet coronal X-ray luminosity L_{XR} is used instead of the stellar luminosity. This is indicated in Fig. 1 which gives a regression plot between $\dot{Y}_{\mathrm{U}}$ and L_{XR}. In addition to the LME data, a dMe star observed by Byrne and McFarland (1980) has been included. The coronal X-ray data was taken from the published work of Johnson (1983), Harris and Johnson (1985) and Ambruster *et al.* (1985) and from unpublished work [J. A. Bookbinder, P. Mayer, L. Golub and R. Rosner (1985, personal communication)].

The line in Fig. 1 represents the linear relation $\dot{Y}_{\mathrm{U}} = 0\cdot 04 L_{\mathrm{XR}}$ and was drawn to represent a reasonable fit to the data.† No effort was made at this stage to make a

* Paper presented at the R. G. Giovanelli Commemorative Colloquium, Part II, Tucson, Arizona, 17–18 January 1985.

† A similar linear correlation between L_{XR} and $\dot{Y}_{\mathrm{U}}$ has also been recently proposed (31 January 1985), independent of the present author (see Doyle and Butler 1985).

0004-9506/85/060971$02.00

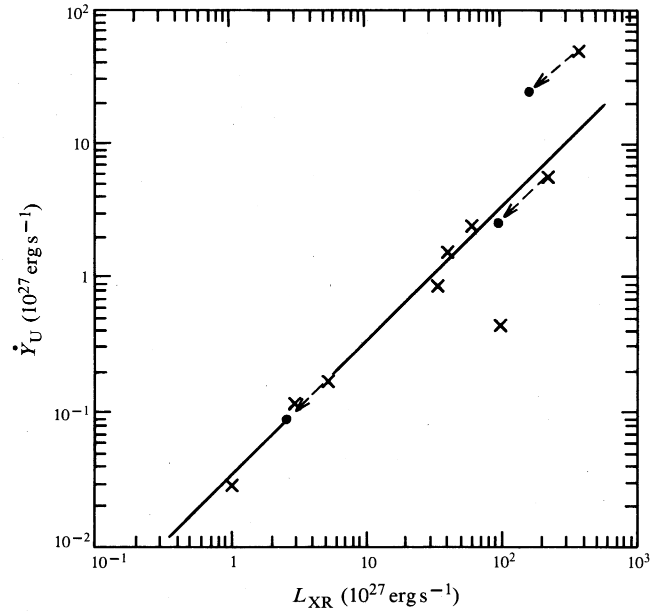

Fig. 1. Regression of the average U-band flare power loss or luminosity $\dot{Y}_U$, against the quiet coronal X-ray power loss L_{XR}, both in units of 10^{27} erg s^{-1}. Observed values are indicated by crosses and the estimated individual star values by dots.

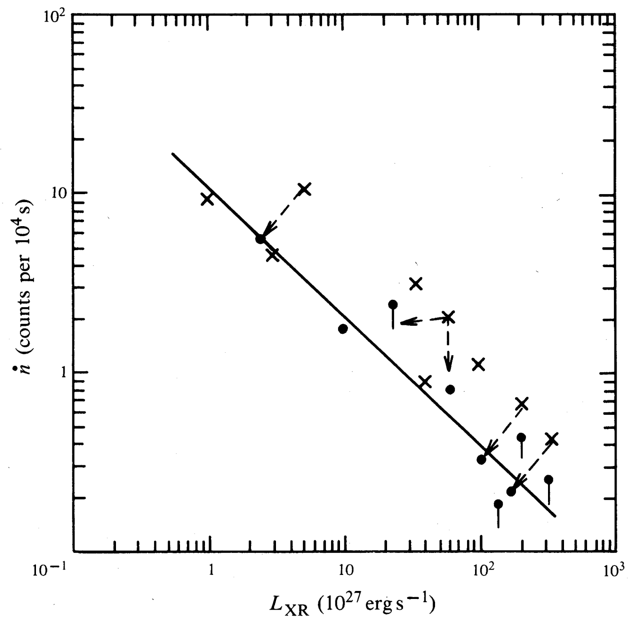

Fig. 2. Regression of the average flare rate $\dot{n}$ per 10^4 s against the quiet coronal X-ray power loss L_{XR}. Observed values are indicated by crosses, the upper limits by a dot with a vertical bar, and the estimated individual star values by dots indicated by arrows.

least squares fit. The two points which significantly deviate represent GLIESE 388 (AD Leo), below the line, and GLIESE 278C, the spectroscopic binary YY Gem.

It is important to consider the effect of duplicity on the regression in Fig. 1. In the case of binaries with essentially similar stars both of which are active, as for YY Gem, the effect of considering individual star values is to shift the unresolved observations, which are plotted by crosses, *parallel* to a linear regression line, as indicated by the arrows for YY Gem (upper right corner) and two other binaries. In the case of binaries with dissimilar stars the effect of going to individual star values would shift the points for each star, if the $\dot{Y}_U(L_{XR})$ relation is truly linear, by different amounts parallel to the linear regression line. Thus, I propose that duplicity will not affect the *linear* regression indicated in Fig. 1 and need not be considered.

The deviation of GLIESE 388 (AD Leo) below the regression line may be, as LME have stated, 'attributed to finite sample effects', since only nine flares in all were detected. However, a total of 19 flares were observed on GLIESE 278C (YY Gem). Without more stars to help define the regression at the upper end we can only conclude that YY Gem deviates for no known reason.

The fact that one can correlate $\dot{Y}_U$ with L_{XR} coupled with the LME correlation cited above implies that L_U correlates with L_{XR} (or vice versa). Such an effect is to be expected if one recalls that Rucinski (1984) showed that L_{XR}/L_{bol}, where L_{bol} is the stellar bolometric luminosity, is essentially a constant in the dMe stars. I suggest that this is because these stars are, similar to Pleiades and post T-Tauri (pre-main-sequence) stars, in a 'saturated' dynamo state. In this state one can expect the maximum conversion of turbulent convective energy*—which is fixed by L_{bol}—into 'topological' magnetic energy, i.e. into fine scale field structure or 'twist'. It is the dissipation of this energy in the corona via 'flaring' that we have in mind.

In Fig. 2 we consider the regression for the mean flare rate $\dot{n}$ on L_{XR}. Here $\dot{n}$ is calculated from the data given by Moffett (1974) and Byrne and McFarland (1980). The upper limits, indicated by a dot with vertical line attached were calculated from null results, where it was assumed that the probability p of the null result in a time interval δt, with $p = \exp(-\dot{n}\delta t)$, was $\geqslant 0{\cdot}5$. The straight line shown corresponding to $L_{XR}^{-2/3}$ is an approximate representation of a portion of the data. Note, however, that the points above the line, representing mostly binaries, define a regression line essentially parallel to the indicated regression.

Here, the issue of duplicity is quite important. Binaries with similar stars, such as YY Gem, are to be translated as indicated by the arrows to yield the (identical) individual star data. These then appear to agree with the indicated regression. In the case of systems with dissimilar stars, such as GLIESE 896AB (at $\dot{n} = 2{\cdot}1\times10^{-4}$ s^{-1}, $L_{XR} = 60\times10^{27}$ erg s^{-1}), the points for the individual stars must be translated in different directions. Only in this case is the partition of $\dot{n}$ between components known. The fainter star (component 896B) contributes 60% to the observed flare frequency (Rodonò 1973). Using the (L_U, L_{XR}) correlation, which I derived for these dMe stars, to obtain the individual L_{XR} values, the results in Fig. 2 are plotted as dots, indicated by arrows from the original location. It appears that both components of GLIESE 896 individually agree with the regression line. The remaining deviant points are GLIESE 285 (YZ CMi) ($\dot{n} = 3{\cdot}2\times10^{-4}$ s^{-1}, $L_{XR} = 34\times10^{27}$ erg s^{-1}) and GLIESE 388 (AD Leo) ($\dot{n} = 1{\cdot}15\times10^{-4}$ s^{-1}, $L_{XR} = 100\times10^{27}$ erg s^{-1}). Could either of these be undetected binaries?

* Rotational energy appears to be too small for this purpose (see Rucinski 1984).

3. Discussion

It appears that the correlation of continuum flare power with quiet coronal X-ray power represents a basic signature of an underlying common magnetic driver for both activity factors. Topological magnetic energy is presumably converted via a 'flare' mechanism into macro-bursts (seen in X rays as well as in the UV continuum as a flare) as well as micro-bursts (i.e. frequent and short lived flares) seen as a quiescent X-ray emission in the corona. It may very well be that quiescent chromospheric emission also owes its origin to micro-bursts (or micro-flares) and represents a thermally reprocessed (or degraded) fraction of the primary energy release, namely high energy electrons.

The suggestion that chromospheric reprocessing of coronal X rays might occur in dMe stars was made by Cram (1982) and corroborated by the recent results reported by Skumanich *et al.* (1985). The latter found that the power loss by the chromosphere in the Balmer-alpha (Hα) line varies *linearly* with the coronal X rays, i.e. $L_{\mathrm{H}\alpha} = 0{\cdot}2 L_{\mathrm{XR}}$, *until* the weak emission state ($\approx 10^{27}$ erg s^{-1}) is reached. For *weak* emitters the evidence suggests that coronal X rays decay secularly at a faster rate than chromospheric emission. Presumably, the opening of closed magnetic regions plays a more significant role for the corona (vis-à-vis coronal holes) than for the chromosphere.

There is currently insufficient data to address the question of the effect of secular evolution out of the saturated dMe state on the relation indicated in Fig. 1. The need to observe dMe (and dM) stars at the same L_{U}, but with different L_{XR}, would help to address this question.

Acknowledgments

The author is grateful to Tom Moffett for sharing his detailed knowledge of flare stars and to Art Young and R. Grant Athay for their comments. He thanks an anonymous referee for clarifying comments.

References

Ambruster, C., Snyder, W. A., and Wood, K. S. (1985). *Astrophys. J.* **284**, 270.
Byrne, P. B., and McFarland, J. (1980). *Mon. Not. R. Astron. Soc.* **193**, 525.
Cram, L. E. (1982). *Astrophys. J.* **253**, 768.
Doyle, J. G., and Butler, C. J. (1985). *Nature* **313**, 378.
Harris, D. E., and Johnson, H. M. (1985). *Astrophys. J.* **294**, 649.
Johnson, H. M. (1983). *Astrophys. J.* **273**, 702.
Lacy, C. H., Moffett, T. J., and Evans, D. S. (1976). *Astrophys. J. Suppl. Ser.* **30**, 85.
Moffett, T. J. (1974). *Astrophys. J. Suppl. Ser.* **29**, 1.
Rodonò, M. (1973). *Boll. Soc. Ital. Fisica* **99**, 95.
Rucinski, S. M. (1984). *Astron. Astrophys.* **132**, L9.
Skumanich, A., Young, A., Stauffer, J., and Bopp, B. W. (1985). *Bull. Am. Astron. Soc.* **16**, 940.

Manuscript received 11 March, accepted 18 June 1985

Aust. J. Phys., 1985, **38**, 975–80

The Eigenvalue Approach in Modelling Solar Magnetic Structures*

Vladimir A. Osherovich

Cooperative Institute for Research in Environmental Sciences,
University of Colorado, and
Environmental Research Laboratories,
National Oceanic and Atmospheric Administration,
325 Broadway, Boulder, CO 80303, U.S.A.

Abstract

A requirement for continuous magnetic fields and finite magnetic energy leads to the eigenvalue approach in magnetohydrodynamics (MHD). Concrete models are developed for sunspots (return-flux sunspot model), prominences, coronal loops and transients. This approach allows a classification of a variety of magnetic topologies and reveals the relations between magnetic and thermodynamic structures. The eigenvalue approach is extended to three-dimensional modelling of the global solar magnetic field.

1. Introduction

In our approach to modelling solar magnetic structures, as long as the kinetic energy density is much smaller than the magnetic energy density ($\frac{1}{2}\rho v^2 \ll B^2/8\pi$), we use the force balance equation

$$(1/4\pi)(\nabla\times \boldsymbol{B})\times \boldsymbol{B} = \nabla P+\rho\nabla F\,, \tag{1}$$

which describes magnetohydrostatic equilibrium. In equation (1), $\boldsymbol{B}$ is the magnetic field which obeys the condition

$$\nabla . \boldsymbol{B} = 0\,, \tag{2}$$

while P and ρ are the gas pressure and density, and F is the gravitational potential. The magnetic force is balanced by the pressure gradient and gravity. Numerous attempts to construct magnetohydrostatic models of sunspots, faculae, prominences, coronal loops and other solar structures have been made since the discovery of magnetic fields on the Sun.

The magnetic force is represented by a nonlinear term in equation (1), which makes it difficult to solve the set (1) and (2). The difficulty disappears if potential or force-free magnetic structures are used as the basis for modelling. For such models,

* Paper presented at the R. G. Giovanelli Commemorative Colloquium, Part II, Tucson, Arizona, 17–18 January 1985.

0004-9506/85/060975$02.00

the magnetic force is zero and the force balance is simply hydrostatic. Then, there is no connection between P and ρ on one side, and $\boldsymbol{B}$ on the other side. However, all observations show that the magnetic field influences thermodynamic parameters in the solar atmosphere.

There is another difficulty with potential and force-free magnetic fields: if not truncated, they represent structures with infinite magnetic energy. Thus, it is necessary to introduce a boundary surface, which separates the domain with the potential (or force-free) field from the outside medium without a magnetic field. This boundary carries surface currents and should be maintained by nonmagnetic forces. In laboratory plasma experiments, these surfaces are made of metal and are maintained by mechanical forces, whereas in the solar atmosphere it is not straightforward to identify these surfaces. Using potential fields, some researchers have identified the sunspot photometric boundary with the magnetic boundary. However, a clearly pronounced magnetic field has been found outside the photometric boundary at distances of up to two sunspot radii [for example, see the magnetogram presented by Osherovich and Lawrence (1983)].

Basically, it is clear that terms like 'singular round sunspot' or 'quiescent solar prominence' refer to a great variety of topologically different configurations [for those concerning prominences see Leroy *et al.* (1984)]. The eigenvalue approach in modelling solar magnetic structures represents a systematic way of obtaining *exact* magnetohydrostatic solutions, which describe topologically different magnetic configurations and provide the basis for their classification. This paper outlines the complete approach, describes the common features of developed two-dimensional models, and presents a new three-dimensional eigenvalue solution of the magnetohydrostatic problem.

2. Requirements for the Magnetic Field

We have two requirements for the magnetic field: (A) the total magnetic energy must be finite, i.e.

$$\iiint \frac{B^2}{8\pi}\,\mathrm{d}V < \infty\,;$$

and (B) the magnetic field must be continuous. These two requirements, taken together, essentially restrict the class of possible magnetohydrostatic solutions. A potential or force-free magnetic field cannot satisfy A and B simultaneously. It has been shown (Osherovich 1975) that these requirements lead to eigenvalue magnetohydrostatic solutions. By considering the influence of the external potential field on our configuration, we require a nonpotential part of the field to obey requirements A and B.

3. Two-dimensional Models

Here we consider modelling the solar magnetic field in cylindrical coordinates (R, z, ϕ), in cartesian coordinates (x, y, z), and in spherical coordinates (r, θ, ϕ). A round singular sunspot can be considered as a magnetic tube, with magnetic and thermodynamic parameters that depend on R and z. Thus, the azimuthal angle ϕ can be ignored. Then, the requirements A and B reduce to the following:

(a1) The magnetic energy density per unit of length of the magnetic tube must be finite, i.e.

$$\iint \frac{B^2}{8\pi} r \, \mathrm{d}r < \infty .$$

(b1) The magnetic field must be continuous in the radial direction.

The return-flux sunspot model (Osherovich 1982*a*) satisfies (a1) and (b1). In this model a surface, which separates magnetic lines going to infinity from those that return back to the Sun, is identified with the umbra–penumbra boundary. Calculations of thermodynamic consequences of this model (Flå *et al.* 1982) support this concept. The return-flux sunspot model is based on the ground-state eigenfunction. The generalization of this model (the double-return-flux sunspot model) developed later by Osherovich and Lawrence (1983) is based on a linear combination of the ground-state and first excited state solutions. The double-return-flux model is capable of describing magnetic lines that return to the Sun twice. Both models also include the self-similar magnetic field of Schlüter and Temesvary (1958) as a special case when there are no magnetic lines that return to the solar surface.

The ribbon-like structure of a quiescent prominence with a typical length of $L \sim 2\times10^5$ km and horizontal width $l \sim (2\text{–}5)\times10^3$ km allows two-dimensional modelling. By considering that in cartesian coordinates, the y direction is along the filament body, we assume that y can be ignored. Then, the requirements A and B reduce to the following:

(a2) The magnetic energy per unit length in the y direction must be finite, i.e.

$$\iint \frac{B^2}{8\pi} \, \mathrm{d}x \, \mathrm{d}z < \infty .$$

(b2) The magnetic field must be continuous in the x–z plane.

The solar prominence model based on eigenvalue solutions (Osherovich 1985*a*) suggests that, besides a simple magnetohydrostatic solution (ground state) which corresponds to a one magnetic body configuration, there are solutions (excited states) that correspond to two-body, three-body etc. configurations. These exact magnetohydrostatic solutions exhibit different density and pressure excess distributions. As a result, of course, temperature profiles are also different. For example, for the ground-state configuration there is a redistribution of density from the lower layer to the higher layer in the solar atmosphere; i.e. the total mass excess is zero. In contrast to the ground-state configuration, the first excited state configuration can maintain a positive mass excess. Much can be learned from studying the influence of the external (potential) field on these localized configurations, because their thermodynamic structure is sensitive to the external field. Especially interesting is the question of the stability of these configurations under the influence of the external magnetic field.

The concept of a continuous magnetic field with finite magnetic energy has been applied to coronal loops and transients. In spherical coordinates a class of analytical axisymmetric MHD solutions that satisfy A and B has been found (Osherovich 1982*b*). The simplest solution describes a toroidal configuration with density excess, concentrated at a certain distance from the centre of the Sun. Observations often show a few coronal loops. Some transients also have two- or three-loop structure. The theoretical interpretation is that excited states are multitoroidal configurations. The excited states correspond to toroids, which are part of the same magnetic configuration and move and change in time, interacting with each other; this is an advantage of the eigenvalue approach. Another advantage is the opportunity to relate local parameters, such as B_{max}, to global parameters, such as the total mass of a transient. The interaction of toroidal currents (described by eigenfunctions) with global potential fields has been studied by Gliner (1984), and the results have enabled the construction of a solar corona model during sunspot minimum (Osherovich *et al.* 1984). The pole–equator asymmetry in this model is explained by the interaction of the global azimuthal current with underlying potential fields. The model is axisymmetric; i.e. the azimuthal angle ϕ can be ignored.

4. Three-dimensional Models

There is sufficient observational evidence (McIntosh 1981; Gaizauskas *et al.* 1983) that the global solar magnetic field is a well-organized three-dimensional structure. In other words, the global solar magnetic field depends on r, θ and ϕ. Therefore, the axisymmetric solutions of the magnetohydrostatic force balance cannot adequately describe the solar magnetic structure. To describe the longitudinal dependence (on ϕ), we must move to three-dimensional modelling.

We note that without gravity ($F = 0$), the Lorentz force is a potential vector (equal to ∇P). In the gravitational field the additional term $\rho \nabla F$ appears on the right side of the force balance equation (1). Now the Lorentz force is a linear combination of a potential vector ∇P and a quasi-potential vector $\rho \nabla F$. We have to search for a magnetic field, which produces the Lorentz force, that is a linear combination of quasi-potential vectors. It can be shown that the magnetic field which is a linear combination of two quasi-potential vectors

$$\boldsymbol{B} = \nabla Q/\alpha + \nabla \Phi/\beta, \tag{3}$$

where Q, Φ, α and β are functions of three variables, corresponds to the magnetic force $(1/4\pi)(\nabla \times \boldsymbol{B}) \times \boldsymbol{B}$, which is a linear combination of quasi-potential vectors (Osherovich 1985*b*). For the case when Q, Φ, α, β and P depend only on two functions (for example on F and Φ), it is possible to reduce the vector equation (1) to one partial differential equation and a complementary condition that allows finding ρ. The three-dimensional field recently considered by Low (1985) in spherical coordinates corresponds to a special case ($\beta = 1$, $Q = r$) of the representation (1). Using the theory of quasi-potential fields (Osherovich 1985*b*) we can obtain the explicit three-dimensional solution of force balance and discuss the possible applications of similar eigenvalue solutions. We assume that

$$\boldsymbol{B} = \nabla \Phi + \frac{\Phi}{D(r)} \nabla r, \tag{4}$$

where D depends only on the radius. Then, in spherical coordinates, equation (1) takes the form

$$\left(-\frac{1}{4\pi D}\frac{\partial \Phi}{\partial r} - \frac{\Phi}{4\pi D^2}\right)\nabla \Phi + \left(\frac{(\nabla \Phi)^2}{4\pi D} + \frac{\Phi}{4\pi D^2}\frac{\partial \Phi}{\partial r}\right)\nabla r = \nabla P + \rho \frac{G M_{\odot}}{r^2}\nabla r. \tag{5}$$

Thus for $P = P(r, \Phi)$ we have

$$-\frac{1}{4\pi D}\frac{\partial\Phi}{\partial r} - \frac{\Phi}{4\pi D^2} = \frac{\partial P(r,\phi)}{\partial\phi}, \tag{6}$$

and the complementary condition

$$\frac{(\nabla\Phi)^2}{4\pi D} + \frac{\Phi}{4\pi D^2}\frac{\partial\Phi}{\partial r} = \frac{\partial P(r,\phi)}{\partial r} + \rho\frac{GM_\odot}{r^2}. \tag{7}$$

Substituting the magnetic field (4) into equation (2) (i.e. $\nabla . \boldsymbol{B} = 0$), we obtain the third equation

$$\Delta\Phi + \frac{1}{D}\frac{\partial\Phi}{\partial r} - \frac{\Phi}{D^2}\frac{\mathrm{d}D}{\mathrm{d}r} = 0. \tag{8}$$

Equation (8) allows us to separate variables, giving

$$\Phi(r,\theta,\phi) = f(r)\mathrm{Y}_{lm} \tag{9}$$

as one of the solutions for equation (8), if

$$\frac{\mathrm{d}}{\mathrm{d}r}\left(r^2\frac{\mathrm{d}f}{\mathrm{d}r}\right) + \frac{1}{D}\frac{\mathrm{d}f}{\mathrm{d}r} - \frac{f}{D^2}\frac{\mathrm{d}D}{\mathrm{d}r} + l(l+1)f = 0, \tag{10}$$

where Y_{lm} is a spherical function. Because equation (8) is linear, we have

$$\partial\Phi/\partial r = C(r)\Phi, \tag{11}$$

where $C(r)$ depends only on the radius. Relation (11) allows us to integrate equation (6), giving

$$P = P_0(r) - \frac{\Phi^2}{8\pi}\left(\frac{C}{D} + \frac{1}{D^2}\right). \tag{12}$$

Then from (7) we find the density

$$\rho = \frac{r^2}{GM_\odot}\left\{-\frac{\mathrm{d}P_0(r)}{\mathrm{d}r} + \frac{(\nabla\Phi)^2}{4\pi D} + \frac{\Phi^2 C}{4\pi D^2} + \frac{\Phi^2}{8\pi}\frac{\mathrm{d}}{\mathrm{d}r}\left(\frac{C}{D} + \frac{1}{D^2}\right)\right\}. \tag{13}$$

If we choose $f(r)$ and $D(r)$ to satisfy (10), we can calculate $C(r)$. Then, the expressions (4), (12) and (13) will give us a three-dimensional magnetohydrostatic solution. We specify $f(r)$, using one of the eigenfunctions of a quantum mechanical oscillator, namely

$$f = f_0(\tfrac{1}{2}r^2 - \tfrac{1}{3}\kappa r^4)\exp(-\kappa r^2), \tag{14}$$

where f_0 and κ are constants. From (10) we find that

$$D(r) = (3-2\kappa r^2)/(14r-4\kappa r^3), \tag{15}$$

and from (11), for $Y_{lm} = Y_{22} = \sin^2\theta \sin 2\phi$, we find that

$$C(r) = (6-14\kappa r^2+4\kappa r^4)/r(3-2\kappa r^2). \tag{16}$$

Thus using these expressions for $C(r)$ and $D(r)$, and with

$$\Phi = f_0(\tfrac{1}{2}r-\tfrac{1}{3}\kappa r^4)\exp(-\kappa r^2)\sin^2\theta \sin 2\phi \tag{17}$$

from (4), we find a three-dimensional magnetic field that is in equilibrium in the atmosphere with pressure, as expressed by (12), and density, as expressed by (13). It is straightforward to check that this magnetic field is continuous everywhere and has a finite magnetic energy. Thus, modified potential fields, namely the class of quasi-potential magnetic fields, can satisfy requirements A and B.

5. Discussion

In many theoretical studies of MHD equations a linearization is used as a first step; for example, this is the usual procedure in the theory of solar oscillations. The solutions of the linearized system can be found as eigenfunctions. We define the eigenvalue approach in MHD as a method of finding *exact* solutions for the original nonlinear system, *without linearizing* the equations. The eigenvalue approach has been proved effective in two-dimensional modelling of solar magnetic structures.

New aspects appear in three-dimensional modelling. The atmosphere with a three-dimensional magnetic field is no longer spherical. The magnetic field modulates gas pressure (see equation 12), density (see equation 13) and temperature. The magnetic field (4) represents magnetic granules, which for a highly conductive plasma can control plasma motions or be affected by these motions.

References

Flå, T., Osherovich, V. A., and Skumanich, A. (1982). *Astrophys. J.* **261**, 700.
Gaizauskas, V., Harvey, K. L., Harvey, J. W., and Zwaan, C. (1983). *Astrophys. J.* **265**, 1056.
Gliner, E. B. (1984). *Astrophys. J.* **283**, 363.
Leroy, J. L., Bommier, V., and Sahal-Brechot, S. (1984). *Astron. Astrophys.* **131**, 33.
Low, B. C. (1985). *Astrophys. J.* **293**, 31.
McIntosh, P. S. (1981). *In* 'The Physics of Sunspots' (Eds L. E. Cram and J. H. Thomas), p. 7 (Sacramento Peak National Observatory: Sunspot, N.M.).
Osherovich, V. A. (1975). *Soln. Dannye (Pulkovo)* No. 8.
Osherovich, V. A. (1982*a*). *Sol. Phys.* **77**, 63.
Osherovich, V. A. (1982*b*). *Astrophys. Space Sci.* **86**, 453.
Osherovich, V. A. (1985*a*). *Astrophys. J.* **297**, 314.
Osherovich, V. A. (1985*b*). *Astrophys. J.* **298**, 235.
Osherovich, V. A., and Lawrence, L. K. (1983). *Sol. Phys.* **88**, 117.
Osherovich, V. A., Tzur, I., and Gliner, B. (1984). *Astrophys. J.* **264**, 412.
Schlüter, A., and Temesvary, S. (1958). *In* 'Electromagnetic Phenomena in Cosmical Physics', IAU Symp. No. 6 (Ed. D. Lehnert), p. 293.

Manuscript received 11 March, accepted 23 September 1985